

UDP-Glucose Dehydrogenase Required for Cardiac Valve Formation in Zebrafish

Emily C. Walsh and Didier Y. R. Stainier*

Cardiac valve formation is a complex process that involves cell signaling events between the myocardial and endocardial layers of the heart across an elaborate extracellular matrix. These signals lead to marked morphogenetic movements and transdifferentiation of the endocardial cells at chamber boundaries. Here we identify the genetic defect in zebrafish *jekyll* mutants, which are deficient in the initiation of heart valve formation. The *jekyll* mutation disrupts a homolog of *Drosophila* Sugarless, a uridine 5'-diphosphate (UDP)-glucose dehydrogenase required for heparan sulfate, chondroitin sulfate, and hyaluronic acid production. The atrioventricular border cells do not differentiate from their neighbors in *jekyll* mutants, suggesting that *Jekyll* is required in a cell signaling event that establishes a boundary between the atrium and ventricle.

Cardiac valves form at chamber boundaries and function to prevent retrograde blood flow through the heart. Extensive work in a chick explant system has revealed some of the cellular interactions necessary for valve formation (1). Endocardial cells at the boundary between the atrium and ventricle are prepatterned to receive a signal from the overlying myocardial cells. This myocardial signal induces the endocardial cells to undergo an epithelial-to-mesenchymal transition, thereby initiating the formation of prevalvular cushions that are later remodeled to form the valves proper. Recent work has implicated transforming growth factor- β family members in the myocardial-to-endocardial signaling event that induces endocardial cushion formation (2–5). However, the mechanism by which myocardial cells at the atrioventricular (AV) boundary acquire the competence to send that signal is not known.

Large-scale screens in zebrafish have identified several mutations that affect cardiac valve formation, the most severe of which is the recessive mutation *jekyll* (6). *jekyll* mutant embryos exhibit pericardial edema and toggling of blood between the two chambers of the heart (compare Fig. 1, A and B). Together these phenotypes are generally indicative of defective AV valve function and are consistent with previous observations that *jekyll* mutant hearts lack valve tissue at 48 hours postfertilization (hpf) (6). To analyze endocardial morphology in vivo, we generated a line of *jekyll* heterozygotes bearing an integrated mouse *tie2* promoter driving green fluorescent protein (GFP) expression in the

developing endocardium (7). In wild-type embryos, endocardial cells cluster at the AV boundary at the onset of valve formation at 43 hpf (Fig. 1C). However, in mutant hearts this clustering fails to occur (Fig. 1D), indicating that *jekyll* function is required for this early endocardial morphogenetic event.

To gain further insight into the *jekyll* valve defect, we isolated the disrupted gene by synteny cloning. We localized *jekyll* to a centromeric region of linkage group 1 using bulk segregant analysis (8) of embryos genotyped for polymorphic CA repeat markers. We then performed fine mapping of the region with 15 polymorphic markers on 200 wild-type haploid embryos and found close linkage between *jekyll* and three of these markers. Next, we genotyped an additional 1150 affected diploid embryos with those three markers as well as for a polymorphism in the 3'-untranslated region of *ldb3* (9). These studies allowed us to further narrow the *jekyll* interval to a 0.5-centimorgan region (Fig. 2A).

Examination of the emerging map of the *jekyll* region revealed a striking conservation of synteny with a region of human chromosome 4p. Taking advantage of this conserved synteny, we mapped four zebrafish expressed sequence tags (ESTs) with sequence similarity to human genes in this 4p region. One of these ESTs, corresponding to a homolog of the *sugarless* gene (known as UDP-glucose dehydrogenase in humans and by convention, referred to as *ugdh* hereafter), was found by radiation hybrid mapping to lie between two markers closely flanking the *jekyll* locus. Sequence analysis of cDNA prepared from wild-type and mutant embryos revealed a T to A change at base pair 992 in the mutant allele. Genotyping for this change revealed no recombination between *jekyll* and the observed lesion in 2870 meioses (Fig. 2, A and B) (10). The T to A change results in an

embedded in paraffin, sectioned (10 μ m), and stained with hematoxylin and eosin. Whole-mount β -galactosidase staining and immunostaining for PECAM-1 (29) and in situ hybridization for PAR1 mRNA (77) and for an SV40 sequence tag in the TIE2p/e-PAR1 transgene mRNA (30) were performed as described.

13. S. Offermanns, C. F. Toombs, Y. H. Hu, M. I. Simon, *Nature* **389**, 183 (1997).
14. G. R. Sambrano, E. J. Weiss, Y. W. Zheng, W. Huang, S. R. Coughlin, *Nature*, in press.
15. R. A. Shivdasani et al., *Cell* **81**, 695 (1995).
16. R. Rugh, *The Mouse: Its Reproduction and Development* (Oxford Univ. Press, New York, 1990).
17. S. J. Soifer, K. G. Peters, J. O'Keefe, S. R. Coughlin, *Am. J. Pathol.* **144**, 60 (1994).
18. Constructs. In the PAR1-LacZ knock-in targeting vector, the start ATG and codons 2 to 4 of PAR1 exon 1 were replaced with a LacZ-PGK-Neo^R cassette. A Kozak sequence immediately preceded the LacZ gene. A 1320-base pair (bp) short arm 5' of the LacZ-PGK-Neo^R cassette, a 4.5-kb long arm 3' of the LacZ-PGK-Neo^R cassette, and a 509-bp Southern probe 5' of the short arm (i.e., outside of the targeting construct) were generated by PCR of BAC DNA containing the PAR1 gene. Primers and Southern analysis were as described in supplementary material (28). The Neo^R cassette was in the same transcriptional direction as PAR1 and was bounded by loxP sites. In vivo cre-mediated excision of the Neo^R cassette using β -actin-cre transgenic mice decreased the intensity of β -galactosidase staining but did not change the overall pattern. For the TIE2p/e-PAR1 transgenic construct a 1.2-kb Eco RI/Xba I (blunted) fragment containing the PAR1 cDNA coding region was inserted 5' to an 847-bp fragment of SV40 small t intron and poly(A) sequence from the vector CPV2 (30) in pBluescript SK (Stratagene). A 2.1-kb Hind III fragment containing the TIE2 promoter and a 9-kb fragment containing the TIE2 enhancer from pHHNS (19) were inserted 5' and 3' to the 2-kb PAR1-SV40, respectively. The resulting 13.1-kb insert was used for microinjections.
19. T. M. Schlaeger et al., *Proc. Natl. Acad. Sci. U.S.A.* **94**, 3058 (1997).
20. T. T. Suh et al., *Genes Dev.* **9**, 2020 (1995).
21. J. H. Erlich et al., *Am. J. Pathol.* **157**, 1849 (2000).
22. M. J. Rabiet et al., *Arterioscler. Thromb. Vasc. Biol.* **16**, 488 (1996).
23. V. Vouret-Craviari, P. Boquet, J. Pouyssegur, E. Van Obberghen-Schilling, *Mol. Biol. Cell* **9**, 2639 (1998).
24. N. E. Tsopanoglou, M. E. Maragoudakis, *J. Biol. Chem.* **274**, 23969 (1999).
25. D. Gospodarowicz, K. D. Brown, C. R. Birdwell, B. R. Zetter, *J. Cell Biol.* **77**, 774 (1978).
26. E. Papadimitriou et al., *Am. J. Physiol.* **272**, C1112 (1997).
27. T. O. Daniel, V. C. Gibbs, D. F. Milfay, M. R. Garovoy, L. T. Williams, *J. Biol. Chem.* **261**, 9579 (1986).
28. Supplementary material is available on Science Online at www.sciencemag.org/cgi/content/full/293/5535/1666/DC1
29. T. M. Schlaeger, Y. Qin, Y. Fujiwara, J. Magram, T. N. Sato, *Development* **121**, 1089 (1995).
30. Y. Srinivasan, F. J. Lovicu, P. A. Overbeek, *J. Clin. Invest.* **101**, 625 (1998).
31. We thank D. Ginsburg of University of Michigan, Ann Arbor, for *FV^{+/-}* mice, J. Degen of Children's Hospital, Cincinnati, for *Fib^{+/-}* mice, T. Sato of University of Texas, Southwestern, for TIE2p/e-LacZ transgenic mice and pHHNS DNA, and G. Martin and B. Black of UCSF for β -actin-cre and smooth muscle α -actin promoter-LacZ transgenic mice, respectively; R. Hamilton and J. Wong for the electron microscopy studies; L. Prentice and R. Advincula for technical assistance; G. Martin, H. Bourne, I. Herskowitz, D. Stainier, and P.-T. Chuang of UCSF for critical reading of this manuscript. C.T.G. was supported by a predoctoral fellowship from the American Heart Association, Western States Affiliate. This work was supported in part by NIH HL44907 and HL65590.

Department of Biochemistry and Biophysics, Programs in Developmental Biology, Genetics and Human Genetics, University of California, San Francisco, CA 94143-0448, USA.

*To whom correspondence should be addressed. E-mail: didier_stainier@biochem.ucsf.edu

2 April 2001; accepted 2 July 2001

REPORTS

Ile-to-Asp substitution at residue 331 (11). Ile-331 is conserved in *Drosophila*, human, and zebrafish Ugdh and is situated in a pocket of nonpolar amino acids in the "hinge" of the omega loop "gate" that allows UDP-glucose access to the active site of the enzyme (Fig. 2C) (12). This Ile-to-Asp substitution is likely to affect enzyme activity.

Ugdh enzymatic activity is required for

the conversion of UDP-glucose into UDP-glucuronic acid, a critical component of hyaluronic acid, heparan sulfate, and chondroitin sulfate glycosaminoglycans (13). Other mutations that affect the production of heparan sulfate proteoglycans in vertebrates result in defects during gastrulation. These include a targeted mouse mutation in the heparan sulfate glycosyltransferase, *EXT1*

(14), and the zebrafish *knypek* mutation, which disrupts a Glypican homolog (15). The *jekyll* mutation, which should affect the production of heparan sulfate at the earliest step in the pathway, shows no obvious phenotype until organogenesis stages. One explanation for this incongruity is that zebrafish *ugdh* mRNA is provided maternally. Indeed, whole-mount in situ hybridization analyses reveal the presence of *ugdh* mRNA at the four-cell stage (11), whereas zygotic transcription begins at the 1000-cell stage. Expression domains in the otic vesicle, heart, and branchial arches in older embryos (30, 37, and 48 hpf, respectively) are consistent with the *jekyll* mutant phenotypes reported here and previously (16).

Morpholino antisense "knockdown" (17) of *ugdh* translation phenocopies the *jekyll* mutation (Fig. 2, D to I). Interestingly, this phenocopy can be achieved only by genetically sensitizing the injected embryos. Such sensitization can be attained in two ways: by halving the maternal product through the use of embryos generated from a cross between a *jekyll* heterozygote female and a wild-type male, in which case 90% of the antisense-injected embryos displayed the *jekyll* phenotype, or by halving the zygotic transcription, i.e., use of embryos from a *jekyll* heterozygote male and a wild-type female, in which case 35 to 50% of the antisense-injected embryos were affected. This sensitization is likely due to the decrease of early ubiquitous maternal and zygotic expression of the *jekyll*

Fig. 1. Comparison of wild-type and *jekyll* mutant heart morphology. Wild-type (A) and mutant (B) embryos at 48 hpf; lateral view, anterior to the left. Pericardial edema surrounds the *jekyll* mutant heart and blood has accumulated in both chambers [at this stage the ventricle is anterior (to the left) and in this embryo, the atrium is slightly obscured by a skin melanocyte]. Arrows point to the heart. *tie2*-GFP allows visualization of wild-type (C) and mutant (D) endocardial morphology at 43 hpf; lateral view, anterior to the top and dorsal to the left. Arrows indicate the AV boundary where endocardial cells cluster in wild-type embryos at the onset of valve formation. wt, wild-type. Bars, 140 μ m.

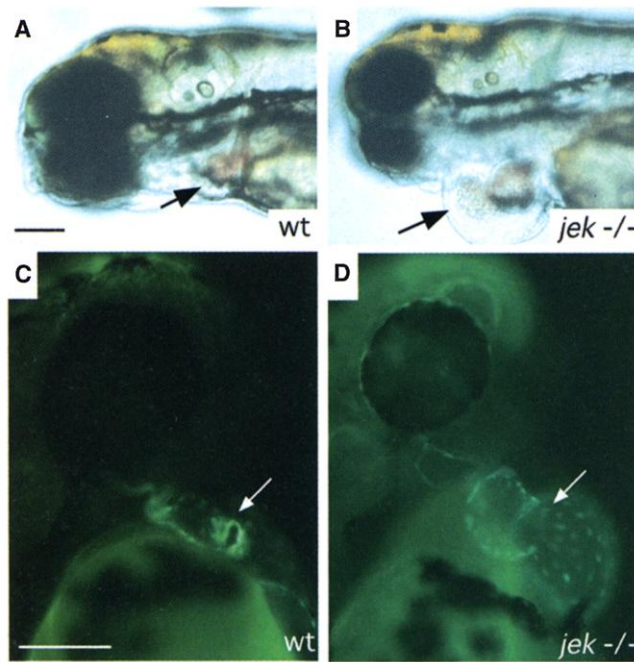
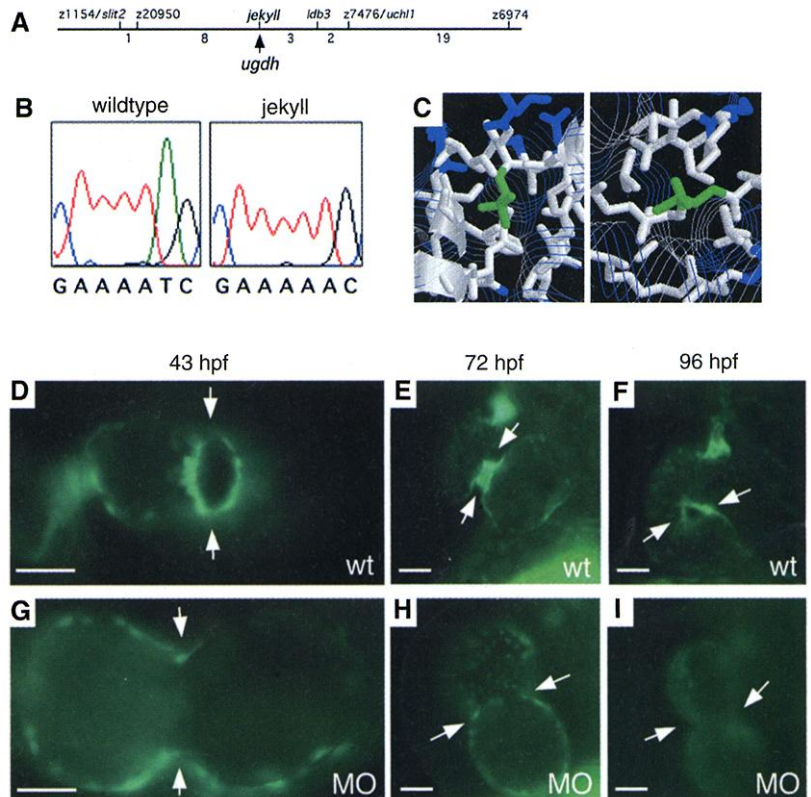


Fig. 2. The *jekyll* locus encodes Ugdh. (A) Integrated genetic and radiation hybrid (RH) maps of the *jekyll* region illustrate the relationships between genes and CA-repeat "z" markers. Numbers below the line indicate the number of recombination events seen in 1150 diploid and 176 haploid embryos tested. Four zebrafish ESTs were chosen for RH mapping because they encode homologs of genes near *SLIT2*, *LDB3*, and *UCHL1* on human chromosome 4p. One of the four, a clone encoding a protein with 84% amino acid identity to human UGDH, maps between *slit2* and *ldb3*, two genes that flank the *jekyll* locus. (B) Sequencing of *ugdh* cDNA revealed a T to A change at base pair 992 in the *jekyll* mutant. This mutation results in an Ile-to-Asp substitution at residue 331. (C) Ile-331 sits in a nonpolar pocket of the enzyme as illustrated in these rasmol images of the bovine UGDH crystal structure (12, 38). The Ile is colored in green, the nonpolar amino acids are in white, and the polar ones are in blue. (D to I) Antisense "knock-down" of *ugdh* phenocopies the *jekyll* mutation [(D to F) uninjected wild-type; (G to I) morpholino-injected]. (D and G) Injection of *ugdh* morpholino into sensitized embryos causes a failure of AV valve formation, here illustrated by a failure of endocardial clustering at the AV boundary in 43 hpf embryos (arrows indicate the AV boundary). Examination at later stages reveals that valve formation does not occur in morpholino-injected embryos, showing that the defect at 43 hpf does not reflect a delay [(E and H) 72 hpf; (F and I) 96 hpf]. wt, wild-type; mo, morpholino-injected. Bars, 20 μ m. The zebrafish *ugdh* cDNA sequence was deposited in GenBank with the accession number AF361478.



gene. The lack of an early phenotype in antisense-injected embryos suggests that in addition to *ugdh* mRNA, Ugdh protein is also provided maternally, or that another protein compensates for the lack of Ugdh, or even that some maternal mRNA is protected from antisense-mediated translational inhibition.

Explant experiments with embryonic chick tissues have shown that valve formation requires precise patterning of the myocardium and endocardium, as well as an inductive signal from the myocardium to the endocardium (1). To determine how *jekyll* affects cardiac valve development, we assessed the expression of early differentiation markers of the valve-forming region: *bone morphogenetic protein (bmp) 4*, *notch1b* (18), and *br146* [a zebrafish *versican* homolog (19)]. Initially all three genes are expressed throughout the anteroposterior extent of the heart. Later expression of these genes is restricted to the valve-forming region (*bmp4* and *br146* in the myocardium at 37 hpf and *notch1b* in the endocardium at 45 hpf). *jekyll* mutant embryos show defects in the expression of these genes (Fig. 3). Although *bmp4* and *br146* expression domains become restricted from the atrium and largely from the ventricle, no heightened expression of these genes is detectable at the AV boundary of *jekyll* mutant hearts at any stage assayed from 36 to 48 hpf (48 hpf shown in Fig. 3, B and D and F and H). *notch1b* expression becomes initially restricted from the atrial endocardium of mutant hearts. However, at

45 hpf, *notch1b* expression is elevated in the AV boundary of wild-type but not *jekyll* mutant embryos (20). At 48 hpf, atrial restriction fails to be maintained in mutant hearts, and *notch1b* expression is again observed throughout the atrial and ventricular endocardium (Fig. 3L). Thus, *jekyll* functions early in the process of AV valve formation and is required specifically in patterning the myocardium and endocardium at the AV boundary. The myocardial patterning defects seen in *jekyll* mutants are likely direct effects of the loss of Jekyll function because they are the first molecular defects to be observed, whereas the later endocardial defects may be secondary to the lack of *bmp4* restriction in the myocardium.

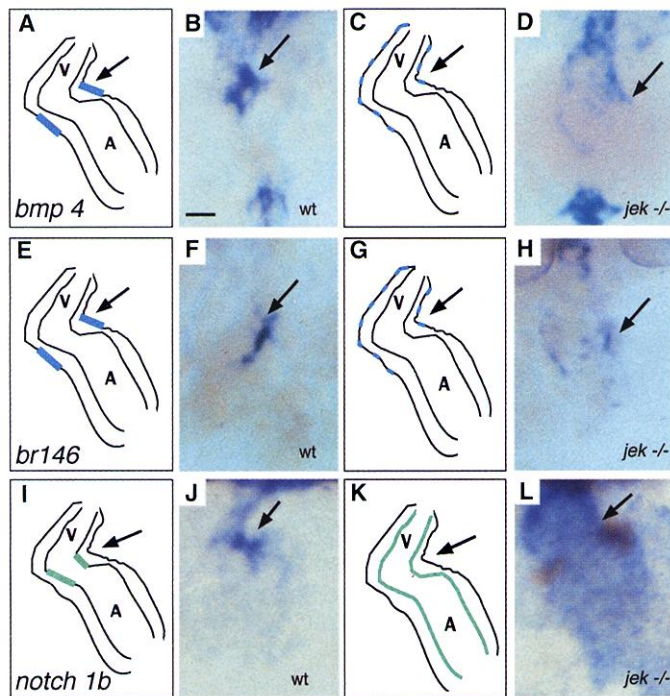
These data lead us to hypothesize that *jekyll* is required for cell signaling events that set aside the valve-forming region as distinct from atrium and ventricle. Perhaps similar to other boundary-formation events in development, the cells at the border between the atrium and ventricle are specified to adopt a tertiary cell fate, that of the valve-forming region. In the *Drosophila* wing disc, for example, differences in *engrailed* expression between the anterior and posterior compartments restrict expression of the Hedgehog signal to the posterior and the Hedgehog receiving apparatus to the anterior. Thus, only cells on the anterior side of the compartment border can receive the Hedgehog signal coming from the posterior (21). A similar situation exists in the

vertebrate limb bud, where differences in *fringe* expression set up a domain of specific Notch signaling at the dorsoventral border (22, 23). The cells at that boundary differentiate to form the apical ectodermal ridge, which is required for further outgrowth of the limb.

Atrial and ventricular fates are properly assigned in *jekyll* mutants, because expression of chamber specific markers appears normal (11). Therefore, the first apparent molecular defect in *jekyll* mutants is a lack of boundary-restricted *bmp4* expression in the myocardium. A similar defect is seen in *cloche* mutant embryos, which lack endocardium altogether (24, 25). Analysis of these two mutants suggests a model in which a primary endocardial signal to the overlying myocardium sets up a border between atrial and ventricular cells. A secondary signal within the myocardium could then produce at the AV boundary a tertiary myocardial cell type with the competence to signal to the underlying endocardium. *jekyll* may be required for the primary endocardial signal or for the secondary myocardial signal that results in the tertiary cell fate.

In *Drosophila*, Sugarless has been shown to be important for Fgf and Wg signaling (26–29). We have analyzed the currently available zebrafish mutations that affect these signaling pathways and have not found any overt defects in cardiac valve formation. By contrast, the similarity of the morphological defects in the formation of the jaw elements in *jekyll*, *pipetail/wnt5a*, and *knypek/glypican* mutants (11, 15) suggests that in this process Jekyll is required for Wnt signaling, and that one substrate for Jekyll is Glypican. In the case of Jekyll's function in the heart, the similarity of the *jekyll* valve phenotype with that seen in mutants for the chondroitin sulfate proteoglycan gene *Versican* (30) suggests that Versican is one substrate for Jekyll in this process. However, mice deficient for *Hyaluronan synthase-2* also exhibit *jekyll*-like valve defects (31), suggesting that *ugdh* may also function in valve formation through its requirement for hyaluronic acid (HA) synthesis. We propose that a signaling pathway, heretofore not identified to require glycosaminoglycan production, depends on Jekyll function during valve formation. Neuregulin is expressed in the ventricular endocardium, and loss of Neuregulin signaling leads to several phenotypes that are also observed in *jekyll* mutants, including the absence of myocardial proliferation in the ventricle and hypoplastic endocardial cushions (31–34). It will be important to investigate the respective role of HA, proteoglycans, and their associated signals during cardiac valve formation.

Fig. 3. Molecular analyses of AV valve development reveal early defects in *jekyll* mutant embryos. Schematized representations are shown to the left of the actual data. Initially expressed throughout the anteroposterior extent of the heart (20), *bmp4*, *br146*, and *notch1b* become restricted to the AV boundary before the onset of valve formation. At 48 hpf, *bmp4* (A and B) and *br146* (E and F) are expressed in the myocardium and *notch1b* (I and J) in the endocardium. RNA in situ hybridization (39) for these genes reveals defects in *jekyll* mutant hearts. (B, D, F, and H) Although expression of *bmp4* and *br146* does become restricted from the atrium and largely from the ventricle, there is no heightened expression at the valve-forming region as in the wild-type. (J and L) *notch1b* expression is not increased at the AV boundary and at this stage is no longer restricted from the atrium. A, atrium; V, ventricle; wt, wild-type. Bar, 20 μ m.



Reversal of Obesity- and Diet-Induced Insulin Resistance with Salicylates or Targeted Disruption of *Ikk β*

Minsheng Yuan,^{1*} Nicky Konstantopoulos,^{1*} Jongsoo Lee,^{1*} Lone Hansen,¹ Zhi-Wei Li,² Michael Karin,² Steven E. Shoelson^{1†}

We show that high doses of salicylates reverse hyperglycemia, hyperinsulinemia, and dyslipidemia in obese rodents by sensitizing insulin signaling. Activation or overexpression of the I κ B kinase β (IKK β) attenuated insulin signaling in cultured cells, whereas IKK β inhibition reversed insulin resistance. Thus, IKK β , rather than the cyclooxygenases, appears to be the relevant molecular target. Heterozygous deletion (*Ikk β ^{+/-}*) protected against the development of insulin resistance during high-fat feeding and in obese *Lep^{ob/ob}* mice. These findings implicate an inflammatory process in the pathogenesis of insulin resistance in obesity and type 2 diabetes mellitus and identify the IKK β pathway as a target for insulin sensitization.

Insulin resistance refers to a decreased capacity of circulating insulin to regulate nutrient metabolism. Individuals with insulin resistance are predisposed to developing type 2 diabetes, and insulin resistance is an integral feature of its pathophysiology. Chronic secretion of large amounts of insulin to overcome tissue insensitivity can lead, in predisposed individuals, to pancreatic β cell failure and concomitant defects in glucose and lipid metabolism. The prevalence of insulin resistance is high and rising, but only rare genetic causes have been identified. The molecular cause of acquired insulin resistance, which is promoted by sedentary lifestyle, obesity, fatty diet, and increased age, and is reversed by exercise and weight loss, is similarly unknown.

High doses of salicylates [4 to 10 g per day (g/day)], including sodium salicylate and aspirin, have been used to treat inflammatory conditions such as rheumatic fever and rheumatoid arthritis. These high doses are thought to inhibit nuclear factor kappa B (NF- κ B) (*I*) and its upstream activator the I κ B kinase β (IKK β) (2), as opposed to working through cyclooxygenases (COXs), the classical targets of nonsteroidal anti-inflammatory drugs (NSAIDs). High doses of salicylates also lower blood glucose concentrations (3–7), although their potential for treating diabetes has been all but forgotten by modern biomedical science. We have investigated potential mechanisms of these hypoglycemic effects to

identify potential mediators of insulin resistance and molecular targets for intervention. We have found that reduced signaling through the IKK β pathway, either by salicylate inhibition or decreased IKK β expression, is accompanied by improved insulin sensitivity in vivo. Our findings further indicate that the IKK β pathway may contribute to insulin resistance in type 2 diabetes and obesity by impinging on insulin signaling.

We determined the effect of high doses of salicylates on the severe insulin resistance seen in genetically obese rodents. Twelve-week-old male Zucker *fa/fa* rats and 8-week-old male *ob/ob* mice were treated for 3 to 4 weeks with 120 mg/kg/day of aspirin or sodium salicylate, administered by continuous subcutaneous infusion. Fasting blood glucose values and glucose tolerance were improved in Zucker *fa/fa* rats (Fig. 1A). Concomitant reductions in insulin concentrations (Fig. 1B) indicated a marked improvement in insulin sensitivity. Glucose tolerance in lean *fa/+* animals was normal, and blood glucose concentrations were similar after aspirin treatment (Fig. 1C). Nevertheless, lower insulin concentrations in the aspirin-treated group (Fig. 1D) demonstrate improved insulin sensitivity, despite milder insulin resistance. The ability of high-dose aspirin to increase insulin sensitivity was further established in insulin tolerance tests (Fig. 1E). Intraperitoneal injection of insulin (2.0 U per kilogram of body weight) had essentially no effect on blood glucose concentrations in untreated *fa/fa* rats. However, the same insulin dose caused a decrease in blood glucose when given to aspirin-treated animals.

Increased triglyceride concentrations in the blood of Zucker rats fell from 494 ± 68 mg/dl to 90 ± 58 mg/dl during 3 weeks of

References and Notes

- L. M. Eisenberg, R. R. Markwald, *Circ. Res.* **77**, 1 (1995).
- C. B. Brown, A. S. Boyer, R. B. Runyan, J. V. Barnett, *Science* **283**, 2080 (1999).
- _____, *Dev. Biol.* **174**, 248 (1996).
- A. S. Boyer et al., *Dev. Biol.* **208**, 530 (1999).
- Y. Nakajima, T. Yamagishi, S. Hokari, H. Nakamura, *Anat. Rec.* **258**, 119 (2000).
- D. Y. Stainier et al., *Development* **123**, 285 (1996).
- L. S. Motoike et al., *Genesis* **28**, 75 (2000).
- J. H. Postlethwait, W. S. Talbot, *Trends Genet.* **13**, 383 (1997).
- Haploid wild-type and diploid mutant embryos from AB/SJD hybrids were genotyped for agarose polymorphisms with z1154, z20950, and z6974, as well as for a single-strand conformation polymorphism (SSCP) (35) in the 3'-untranslated region of *ldb3*.
- The coding sequence mutation in *ugdh* was determined by sequencing wild-type and mutant cDNA clones isolated with primers designed from zebrafish EST sequence information (fc15f10 *ugdh* EST, GenBank accession number Al657608). Mutations were confirmed by dCAP-based RFLP generated by the T to A substitution at base pair 992 using the primers 5'-GACATGAATGAATATCAGAGAAAGAG-3' and 5'-AGGAGAAACCCAAACAACGC-3' and digesting with Mlu I. Oligonucleotides were designed as described (36).
- Supplementary Web material is available on Science Online at www.sciencemag.org/cgi/content/full/293/5534/1670/DC1.
- R. E. Campbell, S. C. Mosimann, I. van De Rijn, M. E. Tanner, N. C. Strynadka, *Biochemistry* **39**, 7012 (2000).
- A. D. Lander, S. B. Selleck, *J. Cell Biol.* **148**, 227 (2000).
- X. Lin et al., *Dev. Biol.* **224**, 299 (2000).
- J. Topczewski et al., *Dev. Cell* **1**, 251 (2001).
- S. C. Neuhauss et al., *Development* **123**, 357 (1996).
- Morpholinos designed against zebrafish *ugdh* (5'-TCTTTTAACTGAAACATCGTGC-3') were injected at 4 ng per embryo.
- J. Westin, M. Lardelli, *Dev. Genes Evol.* **207**, 51 (1997).
- C. Thisse, B. Thisse, *Development* **126**, 229 (1999).
- E. C. Walsh, D. Y. R. Stainier, unpublished data.
- Y. Chen, G. Struhl, *Cell* **87**, 553 (1996).
- C. Rodriguez-Esteban et al., *Nature* **386**, 360 (1997).
- E. Lauffer et al., *Nature* **386**, 366 (1997).
- D. Y. Stainier, B. M. Weinstein, H. W. Detrich, L. I. Zon, M. C. Fishman, *Development* **121**, 3141 (1995).
- C. Kim, D. Y. R. Stainier, unpublished data.
- U. Häcker, X. Lin, N. Perrimon, *Development* **124**, 3565 (1997).
- T. E. Haery, T. R. Heslip, J. L. Marsh, M. B. O'Connor, *Development* **124**, 3055 (1997).
- X. Lin, E. M. Buff, N. Perrimon, A. M. Michelson, *Development* **126**, 3715 (1999).
- R. C. Binari et al., *Development* **124**, 2623 (1997).
- C. H. Mjaatvedt, H. Yamamura, A. A. Capehart, D. Turner, R. R. Markwald, *Dev. Biol.* **202**, 56 (1998).
- T. D. Camenisch et al., *J. Clin. Invest.* **106**, 349 (2000).
- D. Meyer, C. Birchmeier, *Nature* **378**, 386 (1995).
- K. F. Lee et al., *Nature* **378**, 394 (1995).
- M. Gassmann et al., *Nature* **378**, 390 (1995).
- M. Orita, H. Iwahana, H. Kanazawa, K. Hayashi, T. Sekiya, *Proc. Natl. Acad. Sci. U.S.A.* **86**, 2766 (1989).
- M. M. Neff, J. D. Neff, J. Chory, A. E. Pepper, *Plant J.* **14**, 387 (1998).
- D. Yelon, S. A. Horne, D. Y. Stainier, *Dev. Biol.* **214**, 23 (1999).
- M. A. S. Saqi, R. Sayle, *Comput. Appl. Biosci.* **10**, 545 (1994).
- Whole-mount in situ hybridization was performed as described (37). Phenylthiourea (Sigma) was used to inhibit pigmentation in some cases (0.003% w/v).
- We thank T. Kornberg, A. Javaherian, and members of the lab for discussions and comments on the manuscript; E. Chiang, B.-C. Chung, M. Tada, M.-A. Akimenko, C. Thisse, B. Thisse, and M. Lardelli for providing probes; L. Solnica-Krezel for sharing observations before publication; and M. Fishman for the *m151 jekyll* allele. Supported by a Howard Hughes Predoctoral Fellowship (E.C.W.), the Program in Human Genetics Genomics Core Facility at UCSF, and grants to D.Y.R.S. from the Packard Foundation and the NIH (HL54737).

¹Joslin Diabetes Center and Department of Medicine, Harvard Medical School, Boston, MA 02215, USA.
²Department of Pharmacology, University of California, San Diego, La Jolla, CA 92093, USA.

*These authors contributed equally to this work.

†To whom correspondence should be addressed. E-mail: Steven.Shoelson@Joslin.harvard.edu